

## Supplementary Methods

### S1 Self-consistent magnetic moments

The magnetic moment of each particle can be determined by self-consistently solving the system of equations

$$\mathbf{m}_i = \bar{\chi}_i v_i \left[ \frac{\mu_0}{\mu_f} H_z \hat{\mathbf{z}} + H_x \hat{\mathbf{x}} + \sum_{j \in \partial i^{(m)}} \frac{3(\mathbf{m}_j \cdot \hat{\mathbf{r}}_{ij}) \hat{\mathbf{r}}_{ij} - \mathbf{m}_j}{4\pi r_{ij}^3} \right], \quad (1)$$

where  $H_z$  ( $H_x$ ) is the vertical (in-plane) component of the external field in air and  $\partial i^{(m)}$  denotes the set of neighbors of particle  $i$  within a cutoff radius  $r_m$ .

### S2 Image dipoles

The difference in magnetic permeabilities of the ferrofluid ( $\mu_f$ ) and the confining glass ( $\mu_0$ ) results in an additional field felt by the particles.

Consider a point dipole with magnetic moment  $\mathbf{m} = (m_x, m_y, m_z)$  located at  $\mathbf{r} = (x, y, z)$  within the ferrofluid. Let the bottom glass slide be in the plane  $z = 0$  and the coverslip be in the plane  $z = h$ . The field within the ferrofluid at  $\mathbf{r} = (x, y, z)$  is a sum of the magnetic field of the real dipole and the fields of two image dipoles located at  $\mathbf{r}_{\text{im}}^{(1)} = (x, y, 2h - z)$  and  $\mathbf{r}_{\text{im}}^{(2)} = (x, y, -z)$  with magnetic moments (derived using [36, Prob. 5.17])

$$\mathbf{m}_{\text{im}} = \left( \frac{\mu_f - \mu_0}{\mu_f + \mu_0} \right) (m_x, m_y, -m_z). \quad (2)$$

### S3 Potential energy calculations in Supplementary Figure S1

The zero temperature potential energies of seven types of structures observed in experiment were calculated. Energy calculations were performed in the high-field limit, in which the gravitational energy is negligible. Three maximum buckling heights were considered, corresponding to slide to coverslip separations  $h = \sigma_n$ ,  $1.17 \sigma_n$ , and  $1.37 \sigma_n$ .

In calculations in which magnetic moments were self-consistently determined, Supplementary Eq. (1) was solved using the Jacobi method and a cutoff radius of  $r_m = 20.1 \sigma_n$ . Convergence of the energy to within 0.1% was obtained within three iterations. For all cases, the total potential energy per particle was calculated using a cutoff radius of  $r_u = 30.1 \sigma_n$ . The two cutoff radii were chosen so as to minimize computation time while yielding an error of  $\leq 0.1\%$  in the potential energy per particle. The values of the parameters used in calculations are presented in Supplementary Table S1.

The values of  $\varphi$  and  $\chi_B$  were chosen such that the magnetic moments of the magnetic and nonmagnetic particles are equal and opposite when they interact with the external field alone. This results in the checkerboard crystal being stable at  $\theta = 0$  (Fig. 1d). Note that because both the magnetic moments and the dipole energy are functions of the product  $\varphi\chi_B$ , calculations performed with any values of  $\varphi$  and  $\chi_B$  that satisfy the magnetic moment condition above result in identical system energies.

The value of  $\mu_m$  in experiment is not known precisely. For the structures observed experimentally (depicted in Supplementary Fig. S1), energy calculations performed with  $\mu_m = 1.5$  account well for the tilt angles at which transitions should occur.

$\sigma_m$	$2.8 \mu\text{m}$
$\sigma_n$	$3.1 \mu\text{m}$
$\mu_m$	1.5
$\mu_n$	1
$\chi_B$	19.5
$ \mathbf{H}_0 $	12 Oe
$\varphi$	1.0 %
$\psi$	0°
$r_m$	$20.1 \sigma_n$
$r_u$	$30.1 \sigma_n$

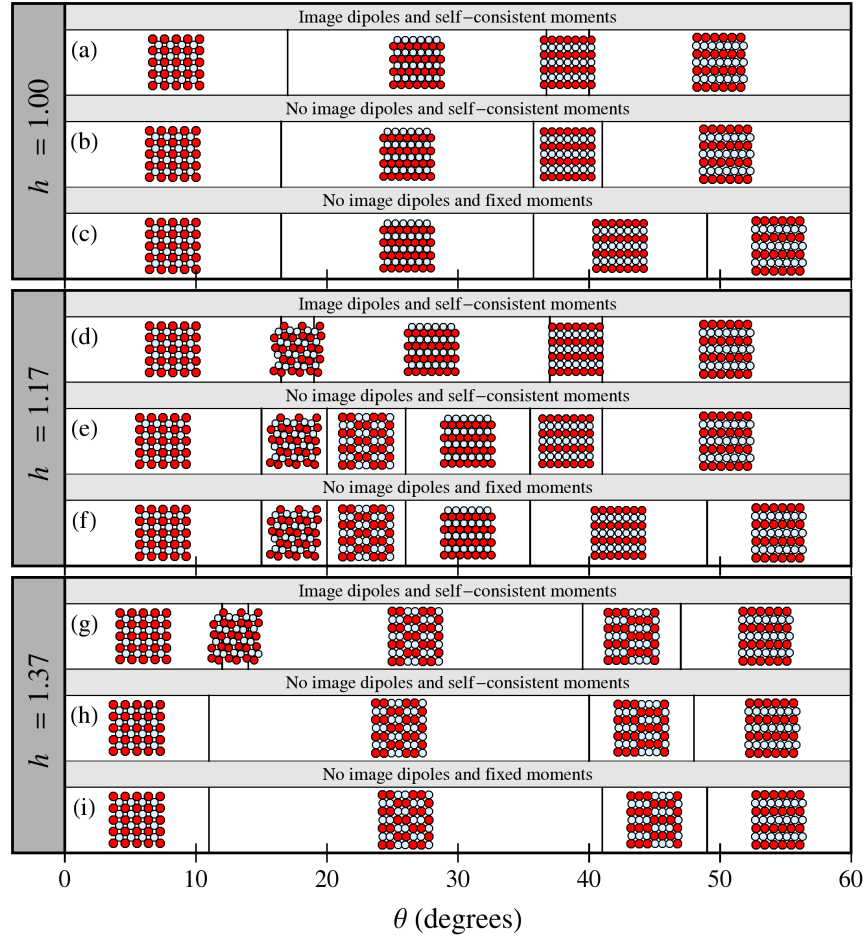
**Supplementary Table S1:** Parameters used in potential energy calculations for Supplementary Fig. S1.

## S4 Simulation Movies of the Martensitic Transformation

Both perfectly two-dimensional and confined three-dimensional systems were considered. In simulations of two-dimensional systems, the particle centers were constrained to only move in the  $z = \sigma_n/2$  plane. In confined three-dimensional systems, the particles were allowed to move between hard walls separated by a distance  $h = 1.11\sigma_n$ . The external field was tilted from 0° to 50° with a tilt rate of 2.5°/2000 MC cycles. To straightforwardly compare the simulation results with the experiments, images and movies were colored using the experimental protocol (See Section 5.4 and the caption for Movie S4).

## References

- [36] John David Jackson. *Classical Electrodynamics*. John Wiley & Sons, 3 edition, 1999.



**Supplementary Figure S1:** Minimal energy structures at various field tilt angles  $\theta$ . Energies were calculated using different values of glass slide to coverslip distance  $h$ . For each buckling height, the effects of including image dipoles and using self-consistently determined magnetic moments was determined. In panels (a), (d), and (g) image dipoles were included and self-consistently determined moments were used. In panels (b), (e), and (h) no image dipoles were included and self-consistently determined moments were used. In panels (c), (f), and (i) no image dipoles were included and the magnetic moments were fixed by the external field only.